water

MDPI

Article

Dissolved Organic Matter in Continental Hydro-Geothermal Systems: Insights from Two Hot Springs of the East African Rift Valley

Andrea Butturini [1,*], Stefano Amalfitano [2,*], Peter Herzsprung [3], Oliver J. Lechtenfeld [4], Stefania Venturi [5], Lydia A. Olaka [6], Nic Pacini [7], David M. Harper [8,9], Franco Tassi [5,10] and Stefano Fazi [2]

1 Department de Biologia evolutiva, Ecologia y Ciencies ambientals, Universitat de Barcelona, 08028 Barcelona, Spain
2 Water Research Institute (IRSA-CNR), Via Salaria km 29.300–CP10, 00015 Monterotondo, Rome, Italy; fazi@irsa.cnr.it
3 Department Lake Research, Helmholtz Centre for Environmental Research (UFZ), 39114 Magdeburg, Germany; peter.herzsprung@ufz.de
4 Department Analytical Chemistry, Research Group BioGeoOmics, Helmholtz Centre for Environmental Research (UFZ), 04318 Leipzig, Germany; oliver.lechtenfeld@ufz.de
5 Department of Earth Sciences, University of Florence, Via G. La Pira 4, 50121 Florence, Italy; stefania.venturi87@gmail.com (S.V.); franco.tassi@unifi.it (F.T.)
6 Department of Geology, University of Nairobi, P.O Box 30197, Nairobi 00100, Kenya; lydiaolaka@uonbi.ac.ke
7 Department of Environmental Engineering, University of Calabria, 87036 Arcavacata di Rende (CS), Italy; nicopacini@gmail.com
8 University of Leicester, Leicester LE1 7RH, UK; dmharper57@googlemail.com
9 Freshwater Biological Association, Ambleside LA22 0LP, UK
10 Institute of Geosciences and Earth Resources (IGG-CNR), Via G. La Pira 4, 50121 Florence, Italy
* Correspondence: abutturini@ub.edu (A.B.); amalfitano@irsa.cnr.it (S.A.)

Received: 26 October 2020; Accepted: 7 December 2020; Published: 14 December 2020

Abstract: Little is known about the quantity and quality of dissolved organic matter (DOM) in waters from continental geothermal systems, with only a few reports available from the Yellowstone US National Park. In this study, we explored the chemodiversity of DOM in water samples collected from two geothermal hot springs from the Kenyan East African Rift Valley, a region extremely rich in fumaroles, geysers, and spouting springs, located in close proximity to volcanic lakes. The DOM characterization included in-depth assessments performed by negative electrospray ionization Fourier-transform ion cyclotron resonance mass spectrometry (FT-ICR-MS). Reduced, saturated and little aromatic DOM compounds were dominant in the hot spring waters collected from either the Ol Njorowa gorge (ON) or the south shore of the soda-saline Lake Elementaita (ELM). Oxygen-poor and sulfur-bearing DOM molecules prevailed in ON, probably reflecting abiotic sulfurization from sulfide-rich geofluids. Nitrogen-bearing aliphatic and protein-like molecules were abundant in ELM, possibly perfusing through the organic-rich sediments of the adjacent Lake Elementaita. Notably, the heat-altered DOM of ancient autochthonous derivation could represent an overlooked source of aliphatic organic carbon for connected lentic environments, with a potential direct impact on nutrient cycling in lakes that receive geothermal water inputs.

Keywords: DOM; FT-ICR-MS; hot springs; East African Rift Valley; Kenya

1. Introduction

Hydrothermal systems are considered active biogeochemical reactors with unique microbial communities and firm candidates for the origin of life [1]. Recent investigations of the carbon cycle in aquatic ecosystems have focused on the role of hydrothermal systems in the synthesis, processing and transformation of dissolved organic matter (DOM), the main carbon and energy source for the abundant heterotrophic fraction of the aquatic microbial community. From a chemical perspective, DOM is a highly complex mixture of thousands of organic molecules which strictly interact with underwater light, selectively absorbing the radiance spectra and minerals through absorption-desorption processes [2,3]. The structural and compositional diversity is known to reflect the DOM origin, persistence and bioavailability for the microbiota [4].

Key literature studies have looked at how the marine DOM is reworked and degraded when recirculating through sub-aquatic hydrothermal vents at oceanic ridges [5], in deep water volcanic mud [6], and in shallow hydrothermal systems [7]. In geothermal fluids under high temperatures, it was reported that oxygen-rich DOM molecules can be selectively removed with the loss of CO_2, carboxyl and hydroxyl groups [8]. Notably, continental geothermal environments were overlooked and, to our best knowledge, a detailed DOM description is available only at Yellowstone Hot Springs [9].

The aims of this study were to (i) provide new data about the chemodiversity of DOM in continental hot springs from a very active geological region, and (ii) compare the DOM properties between continental and marine hydrothermal systems.

We targeted the Kenyan central Rift Valley, a region with a relevant volcanic activity [10], where dozens of hot springs [11] border highly productive saline-alkaline lakes [12]. The DOM properties were analyzed by negative electrospray ionization Fourier-transform ion cyclotron resonance mass spectrometry (FT-ICR-MS) for a molecular-level description of the chemodiversity of DOM extracted through a solid-phase extraction procedure (SPE-DOM).

2. Materials and Methods

2.1. Geological Setting and Sampling Sites

The sampling sites were located in proximity to Lake Naivasha (East African Rift Valley, Kenya). The target area has a high geothermal gradient (>200 °C per km) associated with recent volcanic activity in the area [10]. The groundwater is generally warm (>25 °C), alkaline, and rich in Na^+, K^+, CO_3^{2-}, with a moderately high concentration of F^- anions, which prevent its direct use as a source of drinking water [13,14]. The geology is characterized by comendites, basalts, trachytes and pyroclastics of Pleistocene age, overlain by Holocene volcanites. Soils are moderately alkaline, formed by lacustrine and fluvial sediments [15]. The bedrock is dissected by numerous faults and fractures trending NW-SE, N-S, and E-W, thereby enhancing the permeability of the basin by allowing groundwater to flow through the fractured network [16].

Water samples (approx. 0.5 L at each site) were collected from two hot springs located at the Ol Njorowa gorge (ON, 0°53′48.62″ S; 36°19′8.60″ E, 1860 m a.s.l.) within the Olkaria volcanic high-temperature geothermal field (the largest African geothermal energy field), and at the southern shore of saline-soda Lake Elementaita (ELM, 0°28′22.42″ S, 36°15′29.32″ E, 1776 m a.s.l.). The sample ON was collected from a waterfall flowing over bedrock with patches of a green biofilm. The water temperature was >50 °C (i.e., aquifer temperatures are higher than 150 °C within the geothermal field [16]). The sample ELM was collected from a shallow pool (1 m × 1 m; depth = 0.2 m) on the lakeshore. Water temperature was 36.6 °C and the residence time in the pool was of a few minutes only, because it drained rapidly (approx. 0.3 l/s) towards the lake.

For comparative purposes, an additional four samples were collected from the mixolimnion (from the surface down to 3 m depth) of Lake Sonachi (SO, 0°46′57.68″ S; 36°16″ E, 1891 m a.s.l.), a small (0.18 km^2) meromictic saline-alkaline lake with high DOM concentrations [17]. Lake Sonachi is located in between the two hot springs (34 km from ELM, 15 km from ON) (Figure 1).

Figure 1. Locations of the sampling sites.The yellow arrows pointthe hot springs Ol Njorowa gorge (ON) and Elementaita (ELM). The red star identifies the Lake Sonachi (SO). The red rectangle in the inset figure locates the studied area within the East African Rift Valley.

2.2. Sample Preparation

Filtered samples (300 mL onto combusted GF/F Whatman filters) were acidified to pH 2 (by addition of HCl) and stored in pre-combusted glass bottles for all DOM analyses. Non-acidified aliquots (100 mL) were stored in polyethylene bottles and used for geochemical characterization. Dissolved gases (i.e., CO_2 and CH_4) were sampled in a pre-evacuated 250 mL glass flask, equipped with a Teflon stopcock [18].

2.3. Inorganic Solutes and Gas Analysis

Ion chromatography was used to measure the concentrations of Cl^-, SO_4^{2-}, F^- (761 IC-Metrohm AG®), Na^+, and Ca^{2+} (861 Advanced Compact IC-Metrohm AG®). Trace elements (Mn, Fe, Li and As) were assessed using the PerkinElmer® Optima 8000 ICP-OES. Elemental S^{2-} was assessed as SO_4^{2-} after oxidation with H_2O_2 of CdS resulting from the reaction of ΣS^{2-} with a Cd-NH_3 solution [19]. Acidimetric titration (HCl 0.01 N) was used to estimate the concentrations of HCO_3^- and CO_3^{2-}.

Dissolved CO_2 in the headspace of the sampling flask was measured with a 15A Shimadzu® gas chromatograph, equipped with a thermal conductivity detector. CH_4 was analyzed with a 14 A Shimadzu® gas chromatograph equipped with a flame ionization detector [18].

2.4. Quali-Quantitative Characterization of Dissolved Organic Matter

Dissolved organic carbon (DOC) in filtered and acidified samples (triplicates) was measured by oxidative combustion and infrared analysis (TOC-VCSH analyzer, Shimadzu®, Kyoto, Japan). Considering the instrumental detection limit of 0.3 ± 0.1 ppm, two calibration curves with EDTA standard solutions were used (from 0 to 4 ppm for ELM and ON; from 0 to 20 ppm with 1:10 dilution factor for SO).

The DOM quality was assessed by the Fourier-transform ion cyclotron resonance mass spectrometry (FT-ICR-MS). The two hot spring samples (200 mL filtered and acidified) were processed through 100 mg styrene-divinyl-polymere (PPL) solid-phase cartridges (Agilent®, Waldbronn, Germany). The protocol by Dittmar et al. [20] was adopted to concentrate, desalt, and elute the samples and for preconditioning and drying the cartridges. A blank was treated as a sample to remove the interference of cartridges. The SPE-DOM was eluted with 5 mL methanol and kept frozen until analysis [21]. The solid phase extracted DOM (SPE-DOM) extracts were diluted 1:1 (*v*/*v*) with ultrapure water and analyzed with a FT-ICR mass spectrometer equipped with a dynamically harmonized analyzer cell (Solari XR, Bruker Daltonics Inc.®, Billerica, MA, USA) and a 12 T refrigerated actively shielded superconducting magnet instrument (Bruker Biospin®, Wissembourg, France) located at the ProVIS Centre for Chemical Microscopy (Helmholtz Centre for Environmental Research). Samples were infused by an autosampler at a flow rate of 4 µL/min. For each spectrum, 256 scans (ion accumulation time: 15 ms) were co-added in the mass range 150–3000 *m*/*z* with a 4 Mword time domain. Mass spectra were internally calibrated with a list of peaks (*m*/*z* 250–550, $n > 110$) commonly present in natural organic matter; the mass accuracy after internal linear calibration was better than 0.1 ppm. Peaks were considered when the signal/noise (S/N) ratio was >4.

Formulas were assigned to peaks in the mass range 150–700 *m*/*z*, allowing for elemental compositions $C_{1\text{-}60}H_{1\text{-}120}O_{1\text{-}40}N_{0\text{-}2}S_{0\text{-}1}$ with an error range of ±0.5 ppm, as suggested by Lechtenfeld et al. (2014) [22]. Relative peak intensities were calculated based on the summed intensities of all the assigned peaks in each sample. A relative signal intensity of 0.01% was chosen as the dataset detection limit to compensate for the variability in sensitivity between different measurements. A molecular mass peak formula is referred to as "molecule" in this article although one molecular formula can represent several different structural isomers. Only formulas falling within the range $-10 \leq \text{DBE - O} \leq +10$ (DBE: double bound equivalents) were considered for further data evaluation, as discussed elsewhere [23]. Following the molecular formula identification process, each sample was assessed according to the following descriptors: number of detected molecules (richness), molecular mass, H/C, O/C, N/C, S/C, DBE, modified aromaticity index (AImod) [24], nominal oxidation state of carbon (NOSC) [25]. Except for richness, all the descriptors were calculated for each component and as intensity weighted averages. The ratios H/C, DBE and AImod provided information about the degree of saturation of a molecule (i.e., the number of C-C double bonds) whereas the O/C ratio and NOSC were used as descriptors of the (average) carbon oxidation state [25]. According to the values of the different DOM indicators, DOM molecular classes were divided into: carboxyl-rich alicyclic like molecules (CRAM-like), Aliphatics, Aromatics and Condensed Aromatics (CA), saturated molecules, and nitrogen-rich aliphatic compounds (Table 1). CRAM-like, aliphatic and aromatic molecules were subdivided into O-poor and O-rich molecules if the O/C was <0.5 or ≥0.5, respectively.

Table 1. Molecular categories adopted in this study for describing the molecular diversity of the solid phase extracted DOM (SPE-DOM).

Molecular Class	Compositional Constrains	Source
Carboxyl-rich alicyclic like molecules (CRAM-like)	0.3 < DBE/C < 0.68 0.2 < DBE/H < 0.95 0.77 < DBE/O < 1.75	[26]
Aliphatic	DBE/C < 0.3 H/C > 1	[26]
Aromatic	0.5 ≤ AImod ≤ 0.67	[24]
Condensed Aromatic (CA)	AImod > 0.67	[24]
Saturated molecules	H/C > 2 O/C < 0.9	[5]
N-rich aliphatic molecules	H/C > 1.5 O/C < 0.9 N ≥ 1	[5]

3. Results

3.1. Geochemical Context and DOC Concentration

Both springs had pH > 8, reflecting moderate alkalinity, and a high electrical conductivity (EC = 2.9 mS/cm in ON, EC = 3.2 mS/cm in ELM). Waters from ON were richer in sulfate, manganese, iron, lithium and arsenic compared to those from ELM, in which high concentrations of CO_2 and CH_4 were also detected (Table 2).

Table 2. Geochemical analysis of the waters sampled during the present study.

	pH	CO_2 µmol/L	CH_4 µmol/L	S^{2-} mg/L	$SO_4{}^{2-}$ mg/L	$Ca^2{}_+$ mg/L	Na^+ mg/L	K^+ mg/L	F^- mg/L	Mn µg/L	Fe µg/L	Li µg/L	As µg/L
ON	8.4	n.a.	n.a.	n.a.	144	1.0	478	23	n.a.	70.2	1832	590	87
ELM	9.2	75	548	n.a.	69	10.6	784	29	79.8	5.0	63	253	28
SO	9.7	2.4	156	7.8	106	3.5	2496	327	130	5.3	30	161	45

n.a. = not available.

The concentrations of dissolved organic carbon (DOC) were 1.67 mg C/L (ON) and 0.97 mg C/L (ELM), far lower than those measured at Lake Sonachi (97.5 ± 6.8 mg C/L).

3.2. SPE-DOM

Upon the assignment of formulae, FT-ICR-MS detected 3608, 3892 and 4054 ± 281 SPE-DOM molecules at ELM, ON, and SO, respectively (Supplementary Table S1). A total of 2058 molecules were shared between the three waters (ON ∩ ELM ∩ SO). About 16–17% of the SPE-DOM molecules were exclusive to one of two hot springs. These distinctive compounds contributed in both cases to about 9% of the total signal intensity. About 13–14% of the molecules were detected in the two hot springs, but were missing in SO samples (ON ∩ ELM). The most dissimilar samples were SO and ELM, which shared only 7% of molecules (Table 3).

Table 3. Molecular diversity of the solid phase extracted DOM (SPE-DOM) of samples collected from the two hot springs (ON, ELM) and Lake Sonachi (SO).

Sample Combination	Total	CHO	CHNO	CHOS	CHNOS
ON	879	245	318	223	96
ELM	761	193	460	65	43
SO	1027	347	373	148	159
ON ∩ ELM	510	258	165	84	3
ON ∩ SO	445	124	228	89	4
ELM ∩ SO	279	99	169	8	3
ON ∩ ELM ∩ SO	2058	1276	755	27	0

In terms of relative abundance, the most abundant compositional group in ELM comprised O-poor CRAM-like molecules (35.2%), followed by O-poor aliphatic ones (23%). O-rich aromatics (0.5%) and CA (0.6%) compounds were less abundant. An outstanding feature of SPE-DOM from ELM was the high occurrence of N-rich aliphatic compounds (12% of relative abundance) in relation to ON and SO (1.1% and 2.6%, respectively) (Figure 2a). The presence of several O-poor CHOS (1 < H/C < 1.5) molecules in ON and many O-poor aliphatic (H/C > 1.5) CHNO molecules was also noted in ELM (Figure 2g).

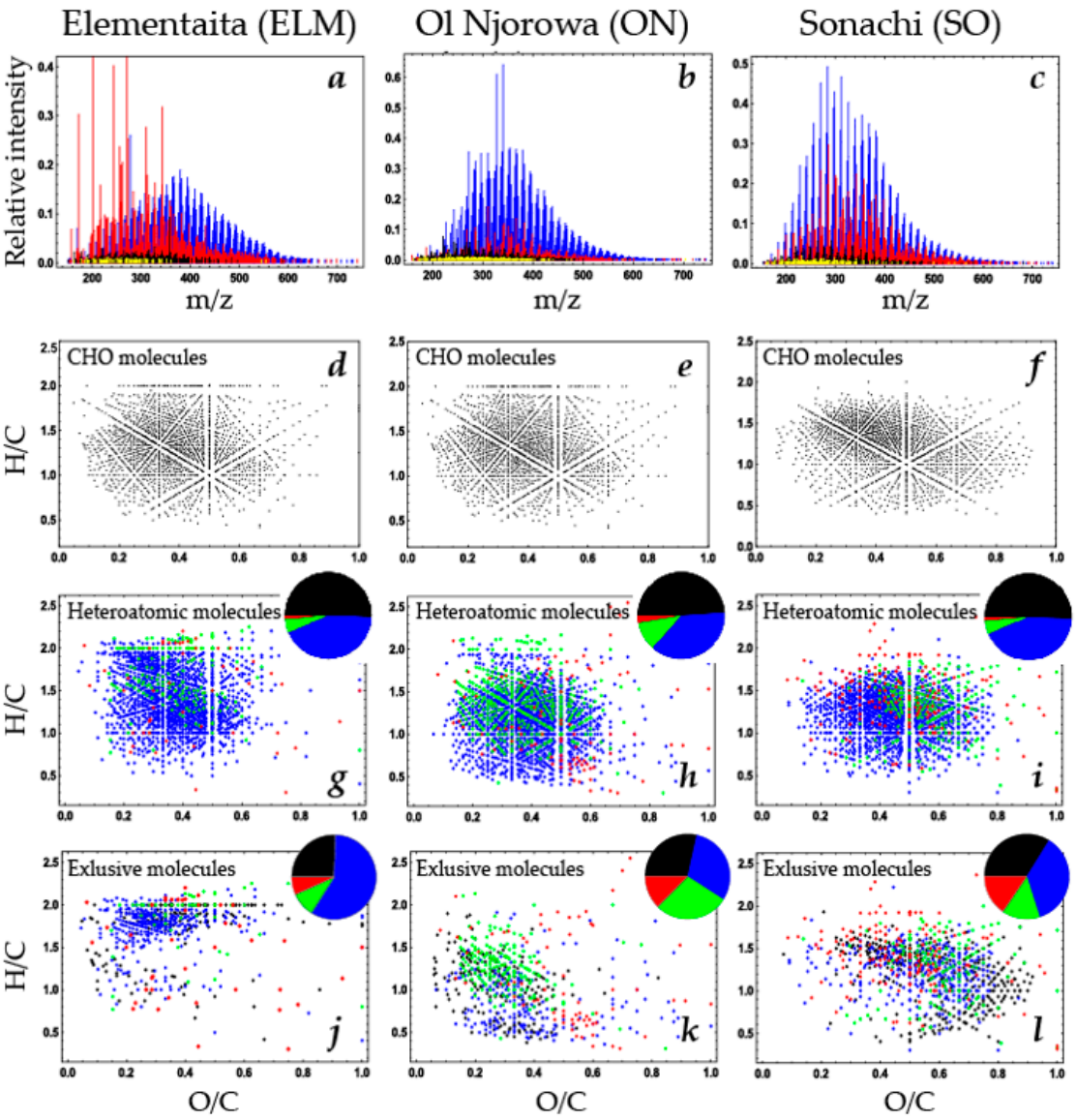

Figure 2. FT-ICR-MS spectra of SPE-DOM, molecular footprints, and associated van Krevelen diagrams for hot springs (ELM, ON) and Lake Sonachi (SO). Colors in the spectra (panels **a–c**) indicate the CRAM-like (blue), CA (yellow), aromatic (black) and aliphatics (red) molecular categories. For better visualization, the van Krevelen diagrams of CHO molecules (**d–f**) are separate from the van Krevelen diagrams of heteroatomic molecules. Pie plots in the van Krevelen diagrams (**g–l**) indicate the frequency of the CHO (black), CHNO (blue), CHOS (green), and CHNOS (red) molecules.

The SPE-DOM from ELM was also visibly more reduced (NOCSw = −0.6; O/C = 0.38), more highly saturated (DBEw = 6.82 and H/Cw = 1.42) and less aromatic (AImod = 0.2) than that from SO. At ON, the relative abundance of aromatics (5.4%) and CA (1.4%) was relevant while the O-rich aliphatics were low (0.6%) (Figure 2b). Overall, SPE-DOM from ON was slightly more reduced (NOCSw = −0.46; O/C = 0.38), more aromatic (AImod = 0.277), and more unsaturated (DBEw = 8.09; H/C = 1.27) than SO (Table 4). Among heteroatomic molecules, the relative abundance of CHNO molecules at ELM (23.4%) was higher than that of SO (18.4%) and ON (10.7%). The relative abundance of S-containing molecules at ON (15.1%) was remarkably greater than at SO (3.5%) and ELM (3.7%) (Figure 2j–l). Furthermore, the relative signal intensity of these S-bearing molecules tended to increase with the increasing number of hydrogen atoms, suggesting the presence of sulfur at a reduced oxidation state in the ON sample (Supplementary Figure S1). At ELM, the exclusive SPE-DOM molecules showed a high

relative intensity of heteroatoms (CHNO, 62%; CHOS, 11%; CHNOS, 4%) (Figure 2j). Almost all the ELM exclusive molecules fell within the category of aliphatics (70.4%); meanwhile, the contribution of CRAM-like, aromatic, and CA molecules, dropped to 4%, 1.4%, and 0.4%, respectively. At ON, the exclusive SPE-DOM was strongly enriched in S-bearing molecules (CHOS, 75.5% and CHNOS, 3.8%, Figure 2k). In a compositional context, the frequency of CRAM-like and O-poor aliphatics strongly decreased, whereas the frequency of CA strikingly increased (Table 4).

Table 4. Molecular characterization of SPE-DOM from the two hot springs (ON, ELM) and Lake Sonachi (SO). Molecular class criteria and SPE-DOM descriptors are defined in Table 1. Percentage values are weighted against relative abundance. All the values are signal intensity weighted. CA: condensed and aromatic.

(**a**)							
	CRAM O-Poor (%)	**CRAM O-Rich (%)**	**CRAM Tot (%)**	**Aliph. O-Poor (%)**	**Aliph. O-Rich (%)**	**Arom. O-Poor (%)**	**Arom. O-Rich (%)**
ON	52.6	9.7	62.3	6.1	0.6	4.4	1.1
ELM	35.2	6.7	41.9	23.0	3.2	3.0	0.5
SO	40.4	18.8	59.2	9.6	2.2	2.4	1.6
Exclusive ELM	3.6	0.5	4.1	8.5	70.4	0	1.4
Exclusive ON	35.9	0.2	36.1	0.4	1.9	2.4	4.3

(**b**)							
	CA (%)	**N-rich Aliphatics (%)**	**Saturated Molecules (%)**	**CHO (%)**	**CHNO (%)**	**CHOS (%)**	**CHNOS (%)**
ON	1.4	1.1	1.1	63.8	10.7	14.7	0.5
ELM	0.6	12.0	4.2	55.4	23.4	3.3	0.4
SO	0.9	2.7	0.1	75.9	18.4	2.4	1.1
Exclusive ELM	0.4	54.7	21.5	22.7	62.2	11.0	4.0
Exclusive ON	6.3	1.7	6.2	9.3	11.4	75.5	3.8

(**c**)								
	NOCSw	**AImodw**	**MassZw**	**DBEw**	**N/Cw**	**S/Cw**	**O/Cw**	**H/Cw**
ON	−0.46	0.28	362.9	8.09	0.010	0.012	0.378	1.274
ELM	−0.60	0.20	368.7	6.82	0.022	0.003	0.376	1.425
SO	−0.32	0.22	356.5	7.11	0.016	0.003	0.465	1.303
Exclusive ELM	−0.93	0.06	375.0	4.20	0.051	0.010	0.330	1.770
Exclusive ON	−0.48	0.29	321.0	8.50	0.017	0.055	0.320	1.290

4. Discussion

The chemodiversity of DOM in geothermal fluids is likely to provide new insights into prebiotic processes occurring in fluid-dependent aquatic environments [27]. Most of the current knowledge is grounded in evidence gathered from deep marine hot springs, while continental hot springs/fumaroles have been largely disregarded [9].

The DOC concentrations estimated at ELM and ON were within the same range of those reported from Yellowstone [28], suggesting that the two samples were not in contact with the lixiviates derived from terrestrial vegetation and soils, nor with the waters of Lake Elementaita that showed extremely high DOC concentrations [29].

Mass spectrometry evidenced that the SPE-DOM from ELM and ON was strongly reduced with an O/Cw ratio in the range of that reported for the Yellowstone hot springs (O/C < 0.4) [9], which was lower than the values typically reported for freshwaters (O/C > 0.45) [30,31]. On the one hand, these results are in agreement with the hypothesis that heat should induce DOM dehydration and the loss of CO_2, carboxyl, and hydroxyl groups [8]. On the other hand, a different pattern was reported for SPE-DOM sampled at deep marine hot vents with an O/Cw ratio higher than 0.4 (Figure 3 and references therein).

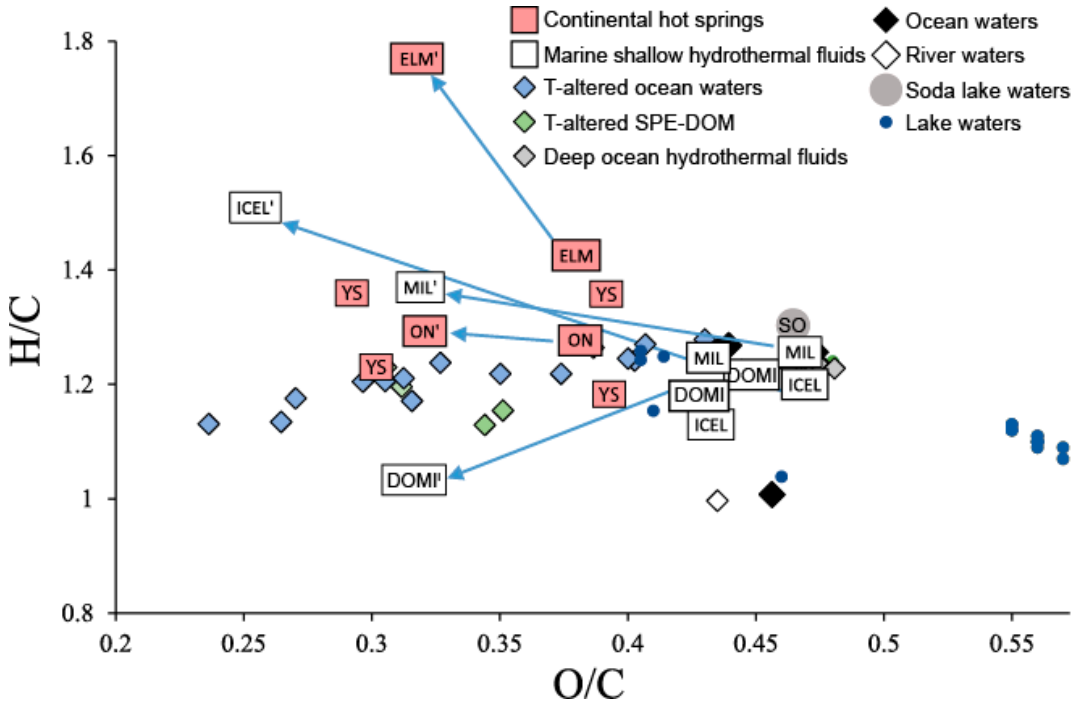

Figure 3. Van Krevelen diagrams showing weighted H/C vs. O/C values (in rectangle) in SPE-DOM samples collected from different hydrothermal systems or altered by heat experiments. Values from freshwater lakes and ocean waters are provided for comparative purposes. Arrows highlight the difference between the weighted O/C and H/C ratios in SPE-DOM from a sample and the same ratios estimated by considering the molecules detected exclusively in that sample. YS: Yellowstone hot springs [9]; MIL: Milos shallow hydrothermal fluids [9]; DOMI: Dominica shallow hydrothermal fluids [7]; ICEL: Iceland shallow hydrothermal fluids [7]; ELM: Elementaita hot spring; ON: Ol Njorowa hot spring. Symbols refer to data collected from deep ocean [5] and Pacific Ocean waters [30], Suwannee River [30], middle ocean ridge hydrothermal fluids [5], thermally altered North equatorial Pacific waters [5], thermally altered SPE-DOM from North Pacific Ocean [8], freshwater lakes [30,31], saline waters from soda Lake Sonachi (SO) [17].

The interaction between the deep (recalcitrant) marine SPE-DOM within hydrothermal systems did not appear to alter substantially the O/C ratio. Yet, an analysis of the unique SPE-DOM described in shallow marine vents [7] revealed that their molecules were clearly more reduced with an O/Cw ratio almost identical to that measured in ELM and ON, or that estimated in marine SPE-DOM exposed to experimental heat alteration [5,8]. Based on the few case studies reported, a generalized tendency towards a more reduced SPE-DOM seems to characterize continental hot springs in opposition to offshore deep hydrothermal vents.

Heat is expected to alter significantly the saturation degree (H/C) of SPE-DOM, along with progressive dehydration, the accumulation of aromatic rings, and a reduction in methyl (CH_3^-) groups [8]. Heat-altered SPE-DOM should be more unsaturated (i.e., lower H/C ratio and high DBE). However, changes in the H/Cw ratio are likely more subtle than those in O/Cw (Figure 3). Previous experiments have evidenced little (or almost nonexistent) change towards more unsaturated molecules [5,8] (Figure 3). In those few reports that provide specific information about the H/Cw ratio of these molecules, the change patterns were unclear. For instance, the decrease in the H/Cw ratio is evident exclusively in SPE-DOM molecules found at the Dominica vent (DOMI) only [7]. Higher values were found in this study (either in ON or more noticeably in ELM) and in the SPE-DOM molecules reported in Iceland (ICEL) [7]. In the SPE-DOM from the Yellowstone hot springs, changes in the H/C ratio were likely inconsistent, but the magnitude was not described [9].

The H/Cw value of ELM is the highest reported so far for SPE-DOM in hydrothermal waters. The ELM hot spring is the only site, among those included in Figure 3, located in close proximity to a lake. Saline-alkaline soda lakes from the East African rift are characterized by very high primary production (mainly driven by *Arthrospira* spp. and other cyanobacteria) [32,33]. Their decay and settling induce the accumulation of large amounts of organic matter at the sediment- water interface [34]. Moreover, these lakes can undergo remarkable water level oscillations, and the nearby hot springs are frequently submerged. Cohen and Nielsen [35] reported that the first 12.5 m of lacustrine sediments, generated over the last 10,000 years, from Lake Elementaita consisted of mud with an organic content of 10–20%. Consequently, ELM hot springs may perfuse through organic-rich sediments reintroducing buried organic carbon (mainly aliphatic) into the lacustrine system.

The presence of high amounts of dissolved CH_4 measured at ELM provides a clue to the presence of an active subsurface prokaryotic community. The dissolved CH_4 was one order of magnitude higher than that of CO_2, and several orders of magnitude higher than the values typically reported in hot spring/fumarole fluids [36].

Moreover, it is noteworthy that N-bearing molecules represent almost 60% of those detected in ELM. Although little is known about the occurrence of N-rich molecules in hydrothermal fluids, N-rich molecules are frequent in experimentally heat-altered SPE-DOM [5,8]. High concentrations of amino acids have been reported in hydrothermal fluids from mid ocean ridges [37]. It cannot be excluded that aliphatic N-rich compounds are metabolites produced by interstitial microbiota [38] that thrive in organic-rich sediments within the lakebed. FT-ICR-MS analyses might have underestimated the abundance of aliphatic substances at the ELM hot spring. Raeke et al. [21] reported that PPL sorbents were less efficient in retaining O-poor (O/C < 0.4) and saturated (i.e., H/C > 1.5) molecules. Therefore, even the contribution of aliphatics in the ELM hot spring might have been underestimated.

At ON, the most prominent property of SPE-DOM was the remarkable abundance of sulfur-bearing molecules. The S/Cw ratio detected in this sample, estimated using all the molecules assigned as well as by using uniquely assigned S-bearing molecules, averaged 0.012 and 0.055, respectively. These values were similar to those reported for shallow hydrothermal vents characterized by strong evidence of abiotic sulfurization [7], suggesting that the ON hydrothermal system DOM might be affected by sulfurization together with dehydration. Likewise, the hydrothermal waters from the nearby Olkaria geothermal system are rich in sulfide (from 2 and 18 mg L^{-1}) [16]. This information corroborates the evidence of H_2S-rich geothermal fluids, together with high temperature and pressure, might facilitate DOM sulfurization.

5. Conclusions

The occurrence of hot springs across the eastern African rift valley provides the opportunity to improve our understanding on how DOM properties may change under high temperature and pressure. Our study revealed the distinctive compositional footprints of heat-modified solid phase-extracted DOM. The signature from two hot springs indicated the accumulation of small- sized O-poor DOM as a consequence of dehydration, the loss of CO_2, and the degradation of carboxyl (COOH) and alcohol/hydroxyl (OH^-) groups. Moreover, we highlighted the potential impact of hydrothermal fluids in introducing heat-altered DOM of ancient autochthonous derivation in lakes with adjacent hot springs. A better understanding of the origin, age, and fate of such a disregarded DOM source will complement the current knowledge on carbon cycling in lakes from geothermal systems.

Supplementary Materials: The following are available online at http://www.mdpi.com/2073-4441/12/12/3512/s1, Table S1: Complete dataset of FT-ICR-MS analyses. Figure S1: Ol Njorowa Gorge. Distribution of CHO (red dots) and CHOS (black dots) intensity peaks in respect to the number of hydrogen atoms. Distributions are for molecules containing 16 (panel a) and 20 (panel b) carbon atoms respectively. Plots show that the distribution of signal intensities of the CHOS molecules is biased towards larger numbers of hydrogen atoms indicating the presence of sulfur at a reduced oxidation state.

Author Contributions: Conceptualization, A.B. and S.F.; Data curation, A.B., P.H. and O.J.L.; Formal analysis, A.B.; Investigation, A.B., S.A., S.V., N.P., D.M.H., F.T. and S.F.; Methodology, A.B., P.H. and O.J.L.; Supervision, A.B.; Writing original draft, A.B., S.A. and L.A.O.; Writing review and editing, A.B., S.A., P.H., O.J.L., N.P. and S.F. All authors have read and agreed to the published version of the manuscript.

Funding: This study was performed under research clearance permit NACOSTI/P/16/23342/10489 Biodiversity studies in Kenya's Rift Valley, granted by the Government of Kenya. The research activities were funded by the Ministerio de Ciencia, Innovación y Universidades (Project DRYHARHSAL, RTI2018-097950-B-C21) and the European Union 7th Framework Programme (Project No. 603629-ENV-2013-6.2.1-Globaqua).

Acknowledgments: We thank Tina Kuhar for the DOM analysis. We gratefully acknowledge Jan Kaesler for his help with the FT-ICR-MS and the Centre for Chemical Microscopy (ProVIS) at the Helmholtz Centre for Environmental Research, Leipzig (Germany), supported by European Regional Development Funds (EFRE-Europe funds Saxony) and the Helmholtz Association. Special thanks to Lawi Kiplimo facilitating access to the site.

Conflicts of Interest: The authors declare no conflict of interest. The funders had no role in the design of the study; in the collection, analysis, or interpretation of data; in the writing of the manuscript; or in the decision to publish the results.

References

1. Deamer, D.W.; Georgiou, C.D. Hydrothermal Conditions and the Origin of Cellular Life. *Astrobiology* **2015**, *15*, 1091–1095. [CrossRef]
2. Thrane, J.-E.; Hessen, D.O.; Andersen, T. The Absorption of Light in Lakes: Negative Impact of Dissolved Organic Carbon on Primary Productivity. *Ecosystems* **2014**, *17*, 1040–1052. [CrossRef]
3. Elkins, K.M.; Nelson, D.J. Spectroscopic approaches to the study of the interaction of aluminum with humic substances. *Coord. Chem. Rev.* **2002**, *228*, 205–225. [CrossRef]
4. Dittmar, T.; Stubbins, A. Dissolved Organic Matter in Aquatic Systems. In *Treatise on Geochemistry*; Elsevier: Amsterdam, The Netherlands, 2014; pp. 125–156. ISBN 9780080983004.
5. Rossel, P.E.; Stubbins, A.; Rebling, T.; Koschinsky, A.; Hawkes, J.A.; Dittmar, T. Thermally altered marine dissolved organic matter in hydrothermal fluids. *Org. Geochem.* **2017**, *110*, 73–86. [CrossRef]
6. Retelletti Brogi, S.; Kim, J.-H.; Ryu, J.-S.; Jin, Y.K.; Lee, Y.K.; Hur, J. Exploring sediment porewater dissolved organic matter (DOM) in a mud volcano: Clues of a thermogenic DOM source from fluorescence spectroscopy. *Mar. Chem.* **2019**, *211*, 15–24. [CrossRef]
7. Gomez-Saez, G.V.; Niggemann, J.; Dittmar, T.; Pohlabeln, A.M.; Lang, S.Q.; Noowong, A.; Pichler, T.; Wörmer, L.; Bühring, S.I. Molecular evidence for abiotic sulfurization of dissolved organic matter in marine shallow hydrothermal systems. *Geochim. Cosmochim. Acta* **2016**, *190*, 35–52. [CrossRef]
8. Hawkes, J.A.; Hansen, C.T.; Goldhammer, T.; Bach, W.; Dittmar, T. Molecular alteration of marine dissolved organic matter under experimental hydrothermal conditions. *Geochim. Cosmochim. Acta* **2016**, *175*, 68–85. [CrossRef]
9. Gonsior, M.; Hertkorn, N.; Hinman, N.; Dvorski, S.E.M.; Harir, M.; Cooper, W.J.; Schmitt-Kopplin, P. Yellowstone Hot Springs are Organic Chemodiversity Hot Spots. *Sci. Rep.* **2018**, *8*, 14155. [CrossRef]
10. Wheildon, J.; Morgan, P.; Williamson, K.H.; Evans, T.R.; Swanberg, C.A. Heat flow in the Kenya rift zone. *Tectonophysics* **1994**, *236*, 131–149. [CrossRef]
11. McCall, J. Lake Bogoria, Kenya: Hot and warm springs, geysers and Holocene stromatolites. *Earth-Sci. Rev.* **2010**, *103*, 71–79. [CrossRef]
12. Fazi, S.; Butturini, A.; Tassi, F.; Amalfitano, S.; Venturi, S.; Vazquez, E.; Clokie, M.; Wanjala, S.W.; Pacini, N.; Harper, D.M. Biogeochemistry and biodiversity in a network of saline–alkaline lakes: Implications of ecohydrological connectivity in the Kenyan Rift Valley. *Ecohydrol. Hydrobiol.* **2018**, *18*, 96–106. [CrossRef]
13. Olago, D.; Opere, A.; Barongo, J. Holocene palaeohydrology, groundwater and climate change in the lake basins of the Central Kenya Rift. *Hydrol. Sci. J.* **2009**, *54*, 765–780. [CrossRef]
14. Olaka, L.A.; Wilke, F.D.H.; Olago, D.O.; Odada, E.O.; Mulch, A.; Musolff, A. Groundwater fluoride enrichment in an active rift setting: Central Kenya Rift case study. *Sci. Total Environ.* **2016**, *545–546*, 641–653. [CrossRef] [PubMed]
15. Washbourn-Kamau, C.K. Late Quaternary Shorelines of Lake Naivasha, Kenya. *Azania Archaeol. Res. Africa* **1975**, *10*, 77–92. [CrossRef]
16. Omenda, P.A. The geology and structural controls of the Olkaria geothermal system, Kenya. *Geothermics* **1998**, *27*, 55–74. [CrossRef]

17. Butturini, A.; Herzsprung, P.; Lechtenfeld, O.J.; Venturi, S.; Amalfitano, S.; Vazquez, E.; Pacini, N.; Harper, D.M.; Tassi, F.; Fazi, S. Dissolved organic matter in a tropical saline-alkaline lake of the East African Rift Valley. *Water Res.* **2020**, *173*, 115532. [CrossRef]
18. Tassi, F.; Fazi, S.; Rossetti, S.; Pratesi, P.; Ceccotti, M.; Cabassi, J.; Capecchiacci, F.; Venturi, S.; Vaselli, O. The biogeochemical vertical structure renders a meromictic volcanic lake a trap for geogenic CO_2 (Lake Averno, Italy). *PLoS ONE* **2018**, *13*, e0193914. [CrossRef]
19. Montegrossi, G.; Tassi, F.; Vaselli, O.; Bidini, E.; Minissale, A. A new, rapid and reliable method for the determination of reduced sulphur (S^{2-}) species in natural water discharges. *Appl. Geochemistry* **2006**, *21*, 849–857. [CrossRef]
20. Dittmar, T.; Koch, B.; Hertkorn, N.; Kattner, G. A simple and efficient method for the solid-phase extraction of dissolved organic matter (SPE-DOM) from seawater. *Limnol. Oceanogr. Methods* **2008**, *6*, 230–235. [CrossRef]
21. Raeke, J.; Lechtenfeld, O.J.; Wagner, M.; Herzsprung, P.; Reemtsma, T. Selectivity of solid phase extraction of freshwater dissolved organic matter and its effect on ultrahigh resolution mass spectra. *Environ. Sci. Process. Impacts* **2016**, *18*, 918–927. [CrossRef]
22. Lechtenfeld, O.J.; Kattner, G.; Flerus, R.; McCallister, S.L.; Schmitt-Kopplin, P.; Koch, B.P. Molecular transformation and degradation of refractory dissolved organic matter in the Atlantic and Southern Ocean. *Geochim. Cosmochim. Acta* **2014**, *126*, 321–337. [CrossRef]
23. Herzsprung, P.; Hertkorn, N.; von Tümpling, W.; Harir, M.; Friese, K.; Schmitt-Kopplin, P. Understanding molecular formula assignment of Fourier transform ion cyclotron resonance mass spectrometry data of natural organic matter from a chemical point of view. *Anal. Bioanal. Chem.* **2014**, *406*, 7977–7987. [CrossRef] [PubMed]
24. Koch, B.P.; Dittmar, T. From mass to structure: An aromaticity index for high-resolution mass data of natural organic matter. *Rapid Commun. Mass Spectrom.* **2006**, *20*, 926–932. [CrossRef]
25. LaRowe, D.E.; Van Cappellen, P. Degradation of natural organic matter: A thermodynamic analysis. *Geochim. Cosmochim. Acta* **2011**, *75*, 2030–2042. [CrossRef]
26. Stubbins, A.; Spencer, R.G.M.; Chen, H.; Hatcher, P.G.; Mopper, K.; Hernes, P.J.; Mwamba, V.L.; Mangangu, A.M.; Wabakanghanzi, J.N.; Six, J. Illuminated darkness: Molecular signatures of Congo River dissolved organic matter and its photochemical alteration as revealed by ultrahigh precision mass spectrometry. *Limnol. Oceanogr.* **2010**, *55*, 1467–1477. [CrossRef]
27. Schmitt-Kopplin, P.; Hemmler, D.; Moritz, F.; Gougeon, R.D.; Lucio, M.; Meringer, M.; Müller, C.; Harir, M.; Hertkorn, N. Systems chemical analytics: Introduction to the challenges of chemical complexity analysis. *Faraday Discuss.* **2019**, *218*, 9–28. [CrossRef]
28. Ball, B.J.W.; Mccleskey, R.B.; Nordstrom, D.K.; Holloway, J.M.; Survey, U.S.G. Water-Chemistry Data for Selected Springs, Geysers, and Streams in Yellowstone National Park, Wyoming, 2003–2005. *U.S. Dep. Inter. U.S. Geol. Surv.* **2006**.
29. Jirsa, F.; Gruber, M.; Stojanovic, A.; Omondi, S.O.; Mader, D.; Körner, W.; Schagerl, M. Major and trace element geochemistry of Lake Bogoria and Lake Nakuru, Kenya, during extreme draught. *Geochemistry* **2013**, *73*, 275–282. [CrossRef]
30. Kellerman, A.M.; Guillemette, F.; Podgorski, D.C.; Aiken, G.R.; Butler, K.D.; Spencer, R.G.M. Unifying Concepts Linking Dissolved Organic Matter Composition to Persistence in Aquatic Ecosystems. *Environ. Sci. Technol.* **2018**, *52*, 2538–2548. [CrossRef]
31. Dadi, T.; Harir, M.; Hertkorn, N.; Koschorreck, M.; Schmitt-Kopplin, P.; Herzsprung, P. Redox Conditions Affect Dissolved Organic Carbon Quality in Stratified Freshwaters. *Environ. Sci. Technol.* **2017**, *51*, 13705–13713. [CrossRef]
32. Lewis, W. Global primary production of lakes: 19th Baldi Memorial Lecture. *Inl. Waters* **2011**, *1*, 1–28. [CrossRef]
33. Oduor, S.O.; Schagerl, M. Phytoplankton primary productivity characteristics in response to photosynthetically active radiation in three Kenyan Rift Valley saline alkaline lakes. *J. Plankton Res.* **2007**, *29*, 1041–1050. [CrossRef]
34. Verschuren, D. Influence of depth and mixing regime on sedimentation in a small, fluctuating tropical soda lake. *Limnol. Oceanogr.* **1999**, *44*, 1103–1113. [CrossRef]
35. Cohen, A.S.; Nielsen, C. Ostracodes as Indicators of Paleohydrochemistry in Lakes: A Late Quaternary Example from Lake Elmenteita, Kenya. *Palaios* **1986**, *1*, 601. [CrossRef]

36. Chiodini, G.; Marini, L. Hydrothermal gas equilibria: The H_2O-H_2-CO_2-CO-CH_4 system. *Geochim. Cosmochim. Acta* **1998**, *62*, 2673–2687. [CrossRef]
37. Klevenz, V.; Sumoondur, A.; Ostertag-Henning, C.; Koschinsky, A. Concentrations and distributions of dissolved amino acids in fluids from Mid-Atlantic Ridge hydrothermal vents. *Geochem. J.* **2010**, *44*, 387–397. [CrossRef]
38. Lechtenfeld, O.J.; Hertkorn, N.; Shen, Y.; Witt, M.; Benner, R. Marine sequestration of carbon in bacterial metabolites. *Nat. Commun.* **2015**, *6*, 6711. [CrossRef]